Computer Physics Communications 209 (2016) 92–95

Contents lists available at ScienceDirect

Computer Physics Communications

journal homepage: www.elsevier.com/locate/cpc

An efficient algorithm for time propagation as applied to linearized augmented plane wave method

J.K. Dewhurst [a], K. Krieger [a], S. Sharma [a,b,*], E.K.U. Gross [a]

[a] Max-Planck-Institut für Mikrostrukturphysik, Weinberg 2, D-06120 Halle, Germany

[b] Department of physics, Indian Institute for technology-Roorkee, 247667 Uttarkhand, India

ARTICLE INFO

Article history:
Received 16 April 2015
Received in revised form
22 July 2016
Accepted 2 September 2016
Available online 9 September 2016

Keywords:
TD-DFT
Time propagation algorithm
LAPW
Spin-dynamics

ABSTRACT

An algorithm for time propagation of the time-dependent Kohn–Sham equations is presented. The algorithm is based on dividing the Hamiltonian into small time steps and assuming that it is constant over these steps. This allows for the time-propagating Kohn–Sham wave function to be expanded in the instantaneous eigenstates of the Hamiltonian. The method is particularly efficient for basis sets which allow for a full diagonalization of the Hamiltonian matrix. One such basis is the linearized augmented plane waves. In this case we find it is sufficient to perform the evolution as a second-variational step alone, so long as sufficient number of first variational states are used. The algorithm is tested not just for non-magnetic but also for fully non-collinear magnetic systems. We show that even for delicate properties, like the magnetization density, fairly large time-step sizes can be used demonstrating the stability and efficiency of the algorithm.

In the 1990s, light-induced demagnetization in Ni was experimentally demonstrated [1]. The field of femtomagnetism [2] has since grown [3–13] and there is a lot of research to achieve light-induced control of spins. However, the physics of light–spin interactions remains highly debated [14–16] largely because of lack of *ab-initio* calculations. Time-dependent density functional theory (TDDFT) [17], which extends density functional theory into the time domain, is a formally exact *ab-initio* method for describing the real-time dynamics of interacting electrons under the influence of a laser field. In order to study femtomagnetism a fully non-collinear extension of TDDFT is required. Within this extension Kohn–Sham (KS) states need to be treated as Pauli spinors and the magnetization density as an unconstrained vector field. Since such a vector field requires very little energy to alter its direction, a highly precise time-evolution algorithm is required for reliable results.

Such an algorithm is required to propagate the time-dependent Schrödinger equation:

$$i\frac{\partial}{\partial t}\left|\Phi_i(t)\right\rangle = \hat{H}(t)\left|\Phi_i(t)\right\rangle, \tag{1}$$

where $\hat{H}$ is the Hamiltonian and Φ the wave function of interacting electrons. By the virtue of the Runge–Gross theorem [17], one can obtain the exact time-propagation of the density of this fully interacting system by solving single particle time-dependent KS equations. In our particular case, where the orbitals are Pauli spinors, these are

$$i\frac{\partial\psi_j(\mathbf{r},t)}{\partial t} = \left[\frac{1}{2}\left(-i\vec{\nabla}+\frac{1}{c}\vec{A}_{\text{ext}}(t)\right)^2 + v_s(\mathbf{r},t) + \frac{1}{2c}\vec{\sigma}\cdot\vec{B}_s(\mathbf{r},t) + \frac{1}{4c^2}\vec{\sigma}\cdot\left(\vec{\nabla}v_s(\mathbf{r},t)\times -i\vec{\nabla}\right)\right]\psi_j(\mathbf{r},t), \tag{2}$$

where $\vec{A}_{\text{ext}}(t)$ is an external vector potential, $\vec{\sigma}$ are the Pauli matrices and ψ_j are the KS orbitals. The KS effective potential $v_s(\mathbf{r},t) = v_{\text{ext}}(\mathbf{r},t) + v_{\text{H}}(\mathbf{r},t) + v_{\text{xc}}(\mathbf{r},t)$ is decomposed into the external potential v_{ext}, the classical electrostatic Hartree potential v_{H} and the exchange–correlation (XC) potential v_{xc}. Similarly the KS magnetic field is written as $\mathbf{B}_s(\mathbf{r},t) = \mathbf{B}_{\text{ext}}(t) + \mathbf{B}_{\text{xc}}(\mathbf{r},t)$ where $\mathbf{B}_{\text{ext}}(t)$ is an external magnetic field and $\mathbf{B}_{\text{xc}}(\mathbf{r},t)$ is the XC magnetic field. The final term of Eq. (2) is the spin–orbit coupling term.

Some of the important requirements for accurate [18,19] time-propagation algorithm for solving Eq. (2) are (a) stability: the errors do not build up as the system is propagated for longer times, (b) efficiency: time propagation is performed by dividing the total time interval into steps and it is essential for an efficient algorithm to allow for large time steps and (c) unitarity: which is required for maintaining the normalization of the wave function at each time-step. In the following we outline one such algorithm which satisfies

* Corresponding author at: Max-Planck-Institut für Mikrostrukturphysik, Weinberg 2, D-06120 Halle, Germany.
E-mail address: sharma@mpi-halle.mpg.de (S. Sharma).

http://dx.doi.org/10.1016/j.cpc.2016.09.001
0010-4655/

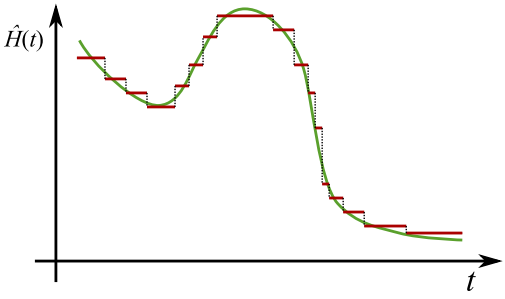

Fig. 1. (Color online) Hamiltonian as a function of time (full line) and approximation to this Hamiltonian (step function).

all the above criteria and is particularly suited for computer codes that deal with dual basis like linearized augmented plane waves (LAPW) and perform exact diagonalization of the Hamiltonian.

The solution of the KS equations can be represented by means of the time evolution operator:

$$|\psi_i(T)\rangle = \hat{U}(T,0)|\psi_i(0)\rangle, \tag{3}$$

where $\hat{U}(T,0)$ is the time evolution operator that propagates all TD-KS states from time $t = 0$ to the final time $t = T$ and satisfies the decomposition law:

$$\hat{U}(T,0) = \hat{U}(T, T-\Delta t)\ldots\hat{U}(2\Delta t, \Delta t)\,\hat{U}(\Delta t, 0) \tag{4}$$

which allows for division of the total time propagation into small steps of step length Δt. In the limit $\Delta t \to 0$ this time propagation operator can be approximated as:

$$\hat{U}(t+\Delta t, t) = e^{-i\hat{h}_s(t)\Delta t}. \tag{5}$$

In principle this exponential expression can be used to stepwise propagate all TD-KS states, in practice however, such an exponential expression of an operator is nearly impossible to calculate exactly (except in certain trivial cases) and iterative schemes like polynomial expansion [20–23], Krylov subspace projection [24,25] and splitting techniques are used [26–34]. All these techniques have been tried and tested, mainly for finite systems, and each one has its own set of advantages and disadvantages [19].

In the present work we propose a method for time propagation in which the Hamiltonian is divided into time steps (Δt) and it is assumed that the Hamiltonian remains constant between time t and $t + \Delta t$ (see Fig. 1). If this can be done then the time evolution operator in the basis of the instantaneous eigenstates of H trivially becomes

$$\hat{U}(t+\Delta t, t) = e^{-i\epsilon(t)\Delta t}, \tag{6}$$

where $\epsilon(t) \equiv \mathrm{diag}(\epsilon_1(t), \ldots, \epsilon_n(t))$ are the instantaneous eigenvalues. Thus if the Hamiltonian can be diagonalized at each time step, the time propagating KS states can be expanded in instantaneous eigenstates of the Hamiltonian. This algorithm is particularly suited for codes where full diagonalization is performed and can be outlined as follows. Let $\chi_i(\mathbf{r})$ be the ground state Kohn–Sham orbitals at $t = 0$ and set $c_{ij}(t=0) = \delta_{ij}$.

1: Set $\psi_j(\mathbf{r}, t) = \sum_i c_{ij}(t)\chi_i(\mathbf{r}), j = 1\ldots N$
2: Compute $\rho(\mathbf{r}, t)$ and $\mathbf{m}(\mathbf{r}, t)$
3: Compute $v_s(\mathbf{r}, t)$, $\mathbf{B}_s(\mathbf{r}, t)$, $\mathbf{A}_s(\mathbf{r}, t)$ to give $\hat{H}(t)$
4: Compute $H_{ij} \equiv \langle\chi_i|\hat{H}(t)|\chi_j\rangle$
5: Solve $H_{ik}a_{kj} = \epsilon_j a_{ij}$ for a and ϵ
6: Compute $c_{ij}(t+\Delta t) = \sum_{kl} a_{ik}\, e^{-i\epsilon_k \Delta t} a^*_{lk} c_{lj}(t), j = 1\ldots N$
7: If $t < T$ goto step 1

Here N is the total number of occupied states, ρ is the charge density and $\mathbf{m}$ is the magnetization density; and the potentials v_s, $\mathbf{B}_s$ and $\mathbf{A}_s$ are functionals of these two densities. All the indices run over all basis states except where indicated. It is important to mention that this algorithm is unitary and thus the KS orbitals are orthonormal at each time-step.

For demonstrating the validity of the algorithm outlined above, various extended systems are studied [35] using the full-potential LAPW method [36] as implemented within the Elk code [37]. The single-electron problem is solved using an augmented plane wave basis without using any shape approximation for the effective potential. Likewise, the magnetization and current densities and their conjugate fields are all treated as unconstrained vector fields throughout space. The deep lying core states (3 Ha below the Fermi level) are treated as Dirac spinors and valence states as Pauli spinors. To obtain the Pauli spinor states, the Hamiltonian containing only the scalar fields is diagonalized in the LAPW basis: this is the first-variational step. The scalar states thus obtained are then used as a basis to set up a second-variational Hamiltonian with spinor degrees of freedom, which consists of the first-variational eigenvalues along the diagonal, and the matrix elements obtained from the external and effective vector fields. This is more efficient than simply using spinor LAPW functions, but care must be taken to ensure there are a sufficient number of first-variational eigenstates for convergence of the second-variational problem. Spin–orbit coupling is also included at this stage.

The second-variational approach is also used for time evolution, namely the coefficients c_{ij} in the algorithm above actually refer to the second-variational states. The first-variational states remain fixed to their ground-state values. This has the advantage of high efficiency but it is essential to check that the number of ground state orbitals is sufficient to accurately describe the evolving orbitals.

Results presented in this work are calculated using a $8 \times 8 \times 8$ **k**-point set for Ni and Diamond and a $6 \times 6 \times 6$ **k**-point set for Fe. 138 Kohn–Sham states per **k**-point were needed to obtain converged results. We have used adiabatic local density approximation (ALDA) for exchange–correlation potential. 1600 time steps per fs were used. This required a computational time of 1.6 s per time step per **k**-point on Intel Xeon E5-2670 v2. This computation time scales linearly with the number of **k**-points and almost quadratically with the number of states.

The efficiency of this algorithm depends upon the step length Δt as well as how easy it is to diagonalize the Hamiltonian in step 5. In the limit $\Delta t \to 0$ the algorithm is exact. It still remains to be seen how large the time step can be chosen so that small errors do not build up as the system is propagated for long times. In order to test this, we first design quantities which will provide a stringent check for efficiency and stability of the algorithm. In the following we present one such quantity,

$$F(t) = \frac{1}{2N}\int d^3r\, |\rho_1(\mathbf{r}, t) - \rho_2(\mathbf{r}, t)|\,, \tag{7}$$

where N is the number of electrons and ρ_1 and ρ_2 are the time-dependent charge densities from two different time propagations of the same Hamiltonian. The difference between these two time propagations is the length of the time step Δt. In the extreme case where the two densities are so different that they do not overlap at any space point then $F(t) = 1$ and if the two densities are exactly the same then $F(t) = 0$. Thus deviation of $F(t)$ from 0 is an indicator of the instability of the algorithm. In Fig. 2 are plotted $F(t)$ for solid Fe under the influence of a time-dependent external vector potential corresponding to an intense laser pulse. The smallest step length used for time propagation was 0.06 attoseconds (as) (this determines the ρ_1). It is clear from these results that the error for step sizes below 5 as are negligible and

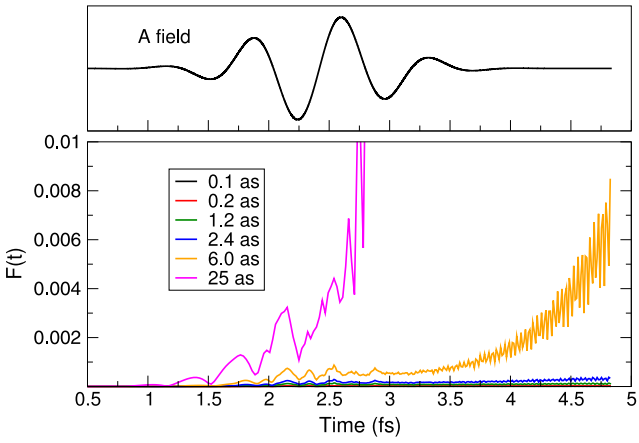

Fig. 2. (Color online) Upper panel: vector potential, $A(t)$, of the applied laser field. Lower panel: function $F(t)$ (as defined in Eq. (7)), for various time steps, as a function of time (in femtoseconds). The laser pulse used has peak intensity of 2×10^15 W/cm^2, frequency of 8.26/fs, fluence of 935 mJ/cm^2 and the pulse is linearly polarized along the x-axis perpendicular to the direction of the spin magnetic moment.

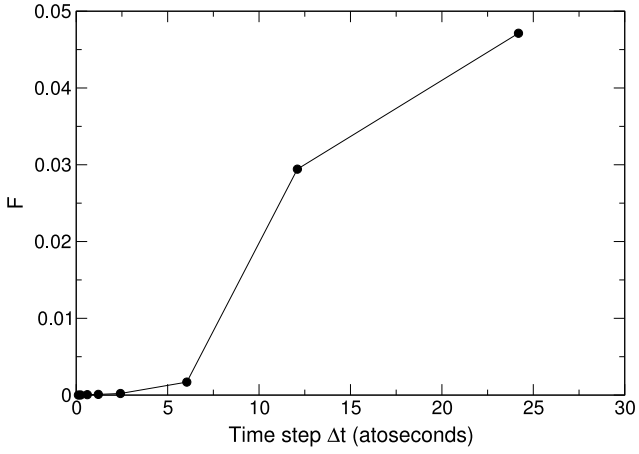

Fig. 3. Function $F(t)$ integrated over time as a function of time step size (Δt).

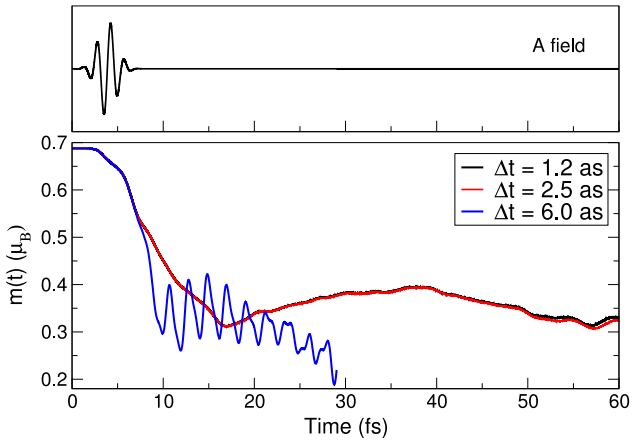

Fig. 4. (Color online) Upper panel: vector potential, $A(t)$, of the applied laser pulse. Lower panel: magnetic moment (in Bohr magnetons) per Ni atom as a function of time (in femtoseconds) for three different time step sizes. The laser pulse used has peak intensity of 2×10^15 W/cm^2, frequency of 4.12/fs, fluence of 935 mJ/cm^2 and the pulse is linearly polarized along the x-axis perpendicular to the direction of the spin magnetic moment.

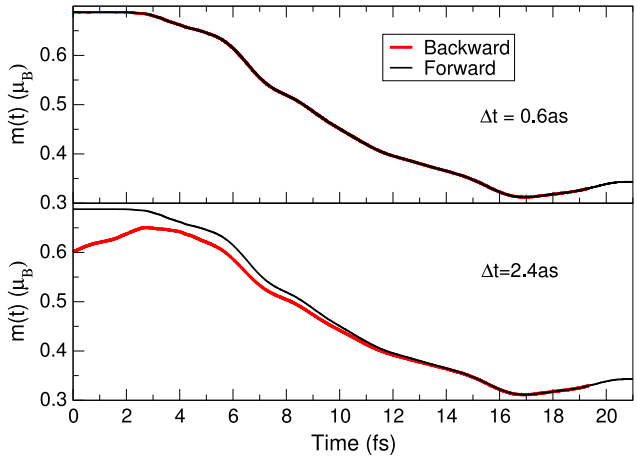

Fig. 5. Magnetic moment (in Bohr magnetons) per Ni atom as a function of time (in femtoseconds) obtained using forward (black) and backward (red) time propagation. Results obtained using two different time steps (upper panel 0.6 as and lower panel 2.4 as) are presented. (For interpretation of the references to color in this figure legend, the reader is referred to the web version of this article.)

can easily be used to obtain reliable results. The errors also do not build up as the system is time propagated over longer times. For step sizes of 6 as or greater, the error is large and builds up as the Hamiltonian is propagated for longer times.

While doing large scale practical calculations, it is difficult to look at quantity like $F(t)$ for each case. It is much more convenient to integrate $F(t)$ over time and look at this single number as a function of Δt. This is plotted in Fig. 3. These results again indicate that time step up to 2.5 as can easily be used. It is important to mention that for studying time-dependent phenomena in the few hundred femtoseconds regime, a typical step size of $\sim$1 as is used. Usually such systems are studied without taking the magnetization density into account, which is much more sensitive quantity than charge density itself. Despite this we find that large step sizes ($\sim$2.5 as) can be used for the time propagation which indicates the stable nature of this algorithm. Similar tests for Diamond (see Fig. 6), a non-magnetic material, reveal that a step size as large as $\sim$6 as can reliably be used.

One can make the test conditions for the algorithm even more stringent by performing similar tests for a fully non-collinear system with spin–orbit coupling [38,39]. Results for the magnetic moment per atoms for solid Ni under the influence of external time-dependent vector potential of an intense laser pulse are shown in Fig. 4. Here the tests are performed for Ni rather than Fe simply because Ni has delocalized electrons with very small moment and is highly sensitive to computational details. The system is non-collinear and undergoes demagnetization due to the presence of spin–orbit coupling term in Eq. (1). The plotted magnetic moment shows that the step size as large as 2.5 as can be used in this case. Not surprisingly, the intensity of the external laser pulse can play an important role in determining the step length. The more intense the pulse the smaller the required step length. To give the algorithm a stringent test, the pulse intensity in the present case is (10^{15} W/cm^2) chosen to be the highest used for such calculations [38,39]. It is important to note that in the present work we have used pulses with wave length in the optical regime. For extreme ultraviolet pulses, obviously, the time step Δt has to be chosen small enough to resolve the wave length.

The time evolution operator satisfies the following relation

$$\hat{U}^{-1}(t + \Delta t, t) = \hat{U}(t, t + \Delta t), \tag{8}$$

a property which is not strictly satisfied in the present algorithm. One may then ask how this affects the time propagation. Since this property of the time evolution operator involves time reversal symmetry, in Fig. 5 we plot the magnetic moment in Ni (same as in Fig. 4) obtained using forward and backward time propagation. It is

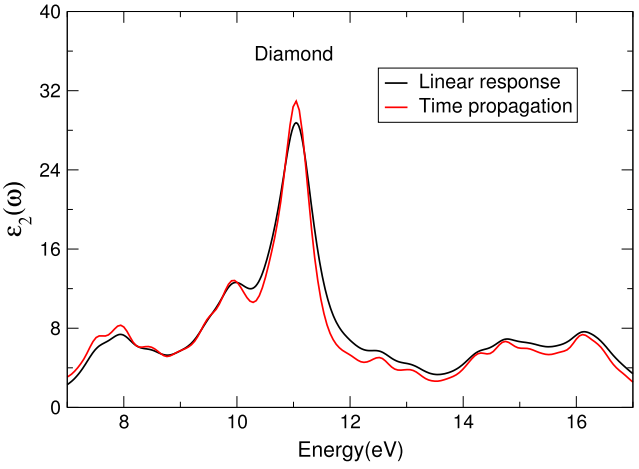

Fig. 6. (Color online) Dielectric function for Diamond as a function of energy (in eV). Results are obtained using linear response (black line) and real time propagation (red line). For obtaining the data shown as red line Kohn–Sham system was time propagated for 500 fs.

clear from Fig. 5 that the error arising from not satisfying Eq. (8) is very small and does not substantially affect the time propagation. Interestingly, we find that even for a time step of 2.4 as, where this error is large (see lower panel Fig. 5), magnetization dynamics is still described accurately (see Eq. (8)).

Yet another test for the robustness of the algorithm is its performance in long time limit (i.e. the stability of the algorithm against error accumulations). This can be tested by performing linear response calculations. The linear response of a system can be calculated in two different ways: (a) using the perturbation theory expression [40,41] and (b) real time propagation under the influence of a small external field. This field has to be small enough to ensure that the system responds linearly. The latter scheme is computational expensive as it requires a time propagation for several 100 s of fs. This is done in order to perform an accurate Fourier transform of the time dependent current to frequency space (for details see Ref. [42]). One can compare the two responses in order to check the robustness of any time propagation scheme. We have done so for the case of Diamond, by time-propagating for 500 fs, and the results are presented in Fig. 6. To give the time propagation algorithm a stringent test the calculations are performed for a large time step of 2.4 as. It is clear from the Fig. 6 that the errors accumulated are indeed very small and the dielectric function is very well reproduced despite the use of large time for time propagation.

To summarize: we present an efficient algorithm for time propagating the Kohn–Sham equations. The algorithm is based on dividing the full time into small time steps and assuming that the Hamiltonian remains constant over each step. This allows for expansion of the time-propagating orbitals in the basis of instantaneous eigenstates of the Hamiltonian. This algorithm is ideally suited for codes where full diagonalization is performed. By performing stringent tests for collinear and non-collinear magnetic systems we demonstrate the efficiency of the algorithm. It is important to emphasize that because the fully unconstrained magnetization vector field requires very little energy to alter its direction, a highly precise time-evolution algorithm is required for reliable results. Present algorithm provides just such precision and stability. A further development of this algorithm would be to include nuclear motion in the time evolution. In this case one would have to incorporate changes in first variational basis since the basis itself depends on the atomic positions. This would require the inclusion of the incomplete basis set corrections, which would be an extension of the work of Yu et al. to the time evolving case [43].

References

[1] E. Beaurepaire, J.-C. Merle, A. Daunois, J.-Y. Bigot, Phys. Rev. Lett. 76 (1996) 4250.
[2] U. Bovensiepen, Nat. Phys. 5 (2009) 461.
[3] J. Hohlfeld, E. Matthias, R. Knorren, K.H. Bennemann, Phys. Rev. Lett. 78 (1997) 4861.
[4] A. Scholl, L. Baumgarten, R. Jacquemin, W. Eberhardt, Phys. Rev. Lett. 79 (1997) 5146.
[5] M. Aeschlimann, M. Bauer, S. Pawlik, W. Weber, R. Burgermeister, D. Oberli, H.C. Siegmann, Phys. Rev. Lett. 79 (1997) 5158.
[6] J. Hohlfeld, J. Güdde, U.C.O. Dühr, G. Korn, E. Matthias, Appl. Phys. B 68 (1999) 505.
[7] H. Regensburger, R. Vollmer, J. Kirschner, Phys. Rev. B 61 (2000) 14716.
[8] L. Guidoni, E. beaurepaire, J.Y. Bigot, Phys. Rev. Lett. 89 (2002) 017401.
[9] A.B. Schmidt, M. Pickel, M. Wiemhöfer, M. Donath, M. Weinelt, Phys. Rev. Lett. 95 (2005) 107402.
[10] A. Kirilyuk, A.V. Kimel, T. Rasing, Rev. Modern Phys. 82 (2010) 2731.
[11] A. Melnikov, I. Razdolski, T.O. Wehling, T.E. Papaioannou, V. Roddatis, P. Fumagalli, O. Aktsipetrov, A.I. Lichtenstein, U. Bovensiepen, Phys. Rev. Lett. 107 (2011) 076601.
[12] M. Sultan, U. Atxitia, A. Melnikov, O. Chubykalo-Fesenko, U. Bovensiepen, Phys. Rev. B 85 (2012) 184407.
[13] C. Stamm, N. Pontius, T. Kachel, M. Wietstruk, H.A. Dürr, Phys. Rev. B 81 (2010) 104425.
[14] B. Koopmans, G. Malinowski, F.D. Longa, D. Steiauf, M. Fähnle, T. Roth, M. Cinchetti, M. Aeschlimann, Nature Mater. 9 (2010) 259.
[15] K. Carva, M. Battiato, P.M. Oppeneer, Nat. Phys. 7 (2011) 665.
[16] G.P. Zhang, W. Hübner, G. Lefkidis, Y. Bai, T.F. George, Nature Phys. Lett. 5 (2009) 499.
[17] E. Runge, E.K.U. Gross, Phys. Rev. Lett. 52 (1984) 997.
[18] C. Molar, C. van Loan, SIAM Rev. 45 (2003) 3.
[19] A. Castro, M.A.L. Marques, A. Rubio, J. Chem. Phys. 121 (2004) 3425.
[20] K. Yabana, G.F. Bertsch, Phys. Rev. B 54 (1996) 4484.
[21] H. Tal-Ezer, R. Kosloff, J. Chem. Phys. 81 (1984) 3967.
[22] R. Baer, R. Gould, J. Chem. Phys. 114 (2001) 3385.
[23] R. Chen, H. Guo, Comput. Phys. Comm. 119 (1999) 19.
[24] T.J. Park, J.C. Light, J. Chem. Phys. 85 (1986) 5870.
[25] M. Hochbruck, C. Lubich, SIAM J. Numer. Anal. 34 (1997) 1911.
[26] M.D. Feit, J.A. Fleck, A. Steiger, J. Comput. Phys. 47 (1982) 412.
[27] M.D. Feit, J.A. Fleck, J. Chem. Phys. 78 (1982) 301.
[28] M. Suzuki, J. Phys. Soc. Japan 61 (1993) L3015.
[29] M. Suzuki, T. Yamauchi, J. Math. Phys. 34 (1992) 4892.
[30] T.Y. Mikhailova, V.I. Pupyshev, Phys. Lett. A 257 (1999) 1.
[31] A.D. Bandrauk, H. Shen, J. Chem. Phys. 99 (1993) 1185.
[32] O. Sugino, Y. Miyamoto, Phys. Rev. B 59 (1999) 2579.
[33] N. Watanabe, T. Tsukada, Phys. Rev. E 65 (2002) 036705.
[34] K.F. Milfeld, R.E. Wyatt, Phys. Rev. A 27 (1983) 72.
[35] Lattice parameter of 3.52 Å for fcc Ni and 2.87 Å for bcc Fe and 3.56 Å for fcc Diamond was used.
[36] D.J. Singh, Planewaves Pseudopotentials and the LAPW Method, Kluwer Academic Publishers, Boston, 1994.
[37] J.K. Dewhurst, S. Sharma, et al., 2004 URL: http://elk.sourceforge.net.
[38] K. Krieger, J.K. Dewhurt, P. Elliott, S. Sharma, E.K.U. Gross, J. Chem Theory Comput. 11 (2015) 4870.
[39] P. Elliott, K. Krieger, J.K. Dewhurst, S. Sharma, E.K.U. Gross, New J. Phys. 18 (2016) 013014.
[40] S. Sharma, J.K. Dewhurst, E.K.U. Gross, Topics in Current Chemistry, 2014.
[41] S. Sharma, J.K. Dewhurst, A. Sanna, E.K.U. Gross, Phys. Rev. Lett. 107 (2011) 186401.
[42] K. Yabana, T. Sugiyama, Y. Shinohara, T. Otobe, G.F. Bertsch, Phys. Rev. B 85 (2012) 045134.
[43] R. Yu, D. Singh, H. Krakauer, Phys. Rev. B 43 (1991) 6411.